Temporal Dynamics of Depression in Premanifest Huntington's Disease: A Network Dysconnection Approach

Tamrin Barta[1], Leonardo Novelli[1], Nellie Georgiou-Karistianis[1], Julie Stout[1], Samantha M Loi[2,3], Yifat Glikmann-Johnston[1], and Adeel Razi[1,4,5,6]

Author affiliations:

[1]Turner Institute of Brain and Mental Health at the School of Psychological Sciences, and, Faculty of Medicine, Nursing and Health Sciences, Monash University

[2]Department of Psychiatry, University of Melbourne.

[3]Neuropsychiatry Centre, Royal Melbourne Hospital, Parkville, Australia

[4]Monash Biomedical Imaging, Monash University, Clayton, Victoria, Australia

[5]Queen Square Institute of Neurology, University College London, London, United Kingdom

[6]CIFAR Azrieli Global Scholars Program, CIFAR, Toronto, Ontario, Canada

Abstract

Depression emerges years before motor signs in Huntington's disease gene expansion carriers (HDGECs)[1–3], yet the neural mechanisms underlying this temporal relationship remain unclear. A growing body of evidence links depression in HDGECs to striatal and default mode network (DMN) regions[4–6], however, the longitudinal evolution of network dysfunction and its relationship to depressive symptoms has not been characterized.

The study included 105 HDGECs (53 Females, M_{age} = 43, Mean CAG repeat length = 43) from the largest longitudinal study of premanifest HD, TrackOn-HD. Here, we applied spectral dynamic causal modelling[7–9] to examine effective connectivity changes over 24 months, alongside voxel-based morphometry of grey matter atrophy and linear mixed models of depressive symptoms, including volumetry.

We show that depression-related network dysconnection operates independently of regional grey matter atrophy, with HDGECs exhibiting widespread striatal volume loss but no differential atrophy patterns between depression groups. Critically, we demonstrate that larger posterior cingulate cortex volumes predicted increased depression severity specifically in HDGECs with depression history, across both Beck Depression Inventory-II (p = .041) and Hospital Anxiety and Depression Scale-Depression Subscale (p = .002). Spectral dynamic causal models explained 88.6% of variance in depression groups and 90.4% in non-depression groups, demonstrating robust model performance. Longitudinal effective connectivity analyses revealed distinct dysconnection profiles: HDGECs with depression history showed widespread interhemispheric alterations including progressive inhibitory changes of striatal-DMN circuits and aberrant hippocampal regulatory control, while those without depression exhibited more focal dysconnection. These patterns occurred despite no group differences in grey matter atrophy trajectories across striatal or cortical regions over the 24-month period. Furthermore, we identify that clinically elevated depressive symptoms associate with differential connectivity patterns of the PCC and hippocampus depending on depression history, suggesting pathological mechanisms become progressively maladaptive.

Our findings challenge the assumption that structural preservation confers functional resilience in neurodegeneration, instead suggesting pathological mechanisms and revealing that functional network reorganization in relatively preserved regions drives depression vulnerability in premanifest HD.

Introduction

Depression emerges early for Huntington's disease (HD) gene expansion carriers (HDGECs)—years before motor signs appear and manifest diagnosis—with psychiatric disturbance preceding motor dysfunction by up to a decade[3]. The trajectory of depression of HD progression remains ambiguous. Depression symptoms are most severe for HDGECs approaching motor diagnosis[1,2], yet prevalence does not increase with disease burden or declining functional capacity[10]. Conversely, depression is linked to cognitive and motor decline[11] and remains elevated throughout HD compared to gene-expansion negative people[12,13]. Within the brain, depression for HDGECs has been linked to structural and functional dysconnection between the default mode network (DMN) and striatum[4–6], however, network disconnection of DMN and striatum longitudinally for HDGECs is still not well characterised. This suggests that network dysconnection could be a neuropathological feature underpinning the relationship between HD progression and depression.

The dorsal striatum—caudate and putamen—degenerates early and severely for HDGECs[14–16], and forms a critical component in frontostriatal circuitry that shows consistent abnormalities in major depression, including volumetric reductions[17] and disrupted network architecture[18,19]. Recent research has suggested outside of the striatum, most other volumetry measurements (total grey and white matter, whole brain volumetry) change meaningfully only 20 years after motor onset[20]. In terms of connectivity, occipital and frontal hyperconnectivity is shown over 20 years from manifest diagnosis[21] which becomes hypoconnectivity as disease burden grows[21,22], and the PCC is proposed as a disease epicentre for HDGECs that develops closer to motor onset, with significant structural connectivity reductions[21]. The DMN serves as a robust neural marker for major depression[23,24], including aberrant functional connectivity between anterior—including medial prefrontal cortex (MPFC)—and posterior DMN—including posterior cingulate cortex (PCC)[25]—, and increased effective connectivity from anterior to posterior regions[26]. This suggests that the pathogenesis of HD confers depression vulnerability for HDGECs.

This network-dysfunction model gains support from Parkinson's disease (PD), where depression also precedes motor signs by several years[27,28], suggesting early depression may represent a shared neurodegenerative mechanism across movement disorders. Like HD, PD depression involves progressive atrophy in DMN regions, including prefrontal cortices, bilateral

hippocampi, and right PCC[29,30]. Crucially, baseline depression severity has predicted faster cortical thinning rates[29], suggesting depression confers risk for greater structural atrophy. PD depression is associated with decreased functional connectivity in frontal regions but increased PCC connectivity, and PCC hyperconnectivity is associated with elevated depressive symptoms[31]. Potential parallels across movement disorders would suggest network dysfunction as a common pathway to early depression vulnerability.

There is conflicting evidence regarding brain change and depression in HDGECs. In terms of atrophy, whole brain or regional volume loss is not associated with broad affective changes[10], and basal ganglia atrophy is not associated with depressive symptoms[32]. By contrast, depression trajectories—across HDGECs and manifest HD—are associated with reduced cortical thickness in limbic regions, prefrontal cortex, and PCC[5]. There is limited research investigating neural dysconnection over HDGEC progression, however, there is evidence that depression is associated with increased functional connectivity within DMN regions (but not in the striatum) and decreased structural connectivity between DMN and basal ganglia[6]. Our recent work[4] investigated effective connectivity aberrations, using spectral dynamic causal modelling (spDCM)[7–9]. For HDGECs with depression history, we found increased inhibitory striatal influence on DMN, including left putamen in line with previous structural findings[33], a propensity for right hippocampal involvement, in line with major depression[34,35], and disinhibitory PCC-hippocampal connectivity in keeping with PCC as a disease epicenter for HD[21]. Our findings suggested posterior DMN as the driver of depression for HDGECs, and potential compensatory mechanisms of right DMN in keeping with compensation in HD broadly[22]. How these directional connectivity patterns evolve over time and relate to depression trajectories remains unknown. We applied spectral dynamic causal modelling (spectral DCM), that uses Bayesian modelling procedure to discriminate both inhibition and excitation of bottom-up and top-down connections, allowing for inference of the direction and strength of connectivity (increased or decreased) between brain regions and within region self-connectivity (i.e., synaptic activity)[36]. Further, the framework measures the association between changes in effective connectivity and behavioral measures[37].

This research focussed on HDGECs, to capture the period where depression appears most influential (prior to motor signs) and to investigate early manifestations of HD. Leveraging the

largest longitudinal dataset (three annual assessments) of HDGECs including structural and functional MRI, TrackOn-HD[10,38], this study examined the temporal dynamics of depression in HDGECs. We hypothesise accelerated grey matter atrophy in regions showing baseline connectivity alterations (left putamen, PCC, hippocampus) in HDGECs who have a history of depression. We hypothesise that baseline grey matter volumes in the DMN will be associated with depression trajectories, with greater grey matter atrophy associated with increased depression symptoms. Further, we hypothesise progressive deterioration in effective connectivity between DMN and striatal regions over time, characterized by disinhibition of striatal regions to DMN hubs and decreased regulatory control from DMN to striatum. Finally, we also hypothesise valence changes (excitation and inhibition) in key network connections (right hippocampus, left putamen, PCC) as disease progresses, with connections becoming increasingly disinhibited as compensatory mechanisms fail.

Materials and methods

Participants

This study used Track-On HD data, with detailed recruitment procedures and protocol previously reported[16,38]. Participants gave written informed consent in accordance with the Declaration of Helsinki and procedures were approved by local ethics committees at all sites. All participants had genetically confirmed to have the HD-causing cytosine, adenine, guanine (CAG) expansion (≥ 39 repeats). Exclusion criteria included history of significant head injury and major neurological disorders (excluding HD) at enrolment[16,38]. HDGECs were not excluded based on medication use, unless part of a therapeutic trial, and were not titrated off medications for study sessions[38]. At each timepoint, comorbid depression and associated International Statistical Classification of Diseases and Related Health Problems 10th Revision (ICD10) classifications were collected and verified by trained clinicians. HDGECs were categorized into two groups based on history of depression (current and remitted) or no history of diagnosed depression. Depression classifications, episode length and number of episodes are reported in Supplementary Results.

Clinical Measures

Three HD-related variables were included in the present study. The CAG repeat length was recorded for each HDGEC. The Unified Huntington's Disease Rating Scale (UHDRS) Total Motor Score (TMS) measured motor sign severity using 15 clinician-assessed items, scoring up to 124 [39]. The CAG-Age Product (CAP) score quantified the effect of age and CAG repeat interaction on disease course ($\mathrm{CAP} = \frac{\text{age} \times (\text{CAG repeat length} - 30)}{6.49}$), and equals 100 at expected diagnosis age[40–43].

Regular (daily) mood medication use was recorded at each time point, including antipsychotics, benzodiazepines, selective serotonin reuptake inhibitors (SSRIs), and non-SSRI anxiolytics and antidepressants. At their first available session, 30 HDGECs were taking mood medications (12 HDGECs with a history of depression), with 25 (83.3%) taking one medication. Consistent with prior HD neuroimaging studies[6,10,16,38,44–47], we included a covariate to account for medication use across all analyses. Medications taken, duration, dose, indication, and regime are reported in Supplementary Table 2.

As a measure of disease burden, the HD Integrated Staging System (HD-ISS) was used[48]. The HD-ISS incorporates pathophysiology alongside clinical and functional changes[48]. This approach extends beyond the current standard of indexing motor impairment for manifest diagnosis [49] by staging disease from 0–3 based on genetic confirmation, striatal volume changes, cognitive impairment, and functional decline[48].

Mood Measures

We included self-report measures to quantify depressive symptoms at each time point: the Beck Depression Inventory-II (BDI-II)[50] and Hospital Anxiety and Depression Scale-Depression subscale (HADS-D)[51]. The BDI-II consists of 21 items with 4-point Likert scaling (maximum score: 63 and higher scores indicate increased depressive symptoms), measured over a two-week period. The BDI-II measures depression symptoms accurately in HD[52] with a cut-off of 10/11 to discriminate clinically elevated depressive symptoms with excellent sensitivity (1.00) and good specificity (0.66)[53]. The HADS-D employs a 4-point Likert scale (maximum score: 21, with higher scores indicating more depressive symptoms)[51]. A cut-off of 6/7 is recommended in HD

for discriminating clinically elevated depression, demonstrating excellent sensitivity (1.00) with good specificity (0.82)[53]. We used these thresholds to categorize HDGECs as endorsing clinically meaningful depressive symptoms at each time-point.

Demographic Analyses

Demographic variables were compared based on depression history using Pearson's Chi-squared test or ANOVA. Assumptions testing was undertaken and is reported in the supplementary materials; minor violations of non-normality were considered acceptable as assumptions were not connected to main analyses.

Statistical Analyses

MRI Data Acquisition

3T structural (T1) and resting-state functional MRI (fMRI) data over three annual sessions (baseline, 12-month, and 24-month follow-up) were acquired on two different scanner types at four sites: Philips Achieva (Vancouver and Leiden) and Siemens TIM Trio (London and Paris). Acquisition procedures are outlined in supplementary materials.

Functional MRI Pre-processing

Pre-processing was performed for all available data using *fMRIPrep* v21.02.2[54,55], MRIQC v22.0.6[56], and FreeSurfer v-6.0.1[57]. The pipeline included slice-timing correction, realignment, spatial normalization to Montreal Neurological Institute (MNI) space, and spatial smoothing with a 6 mm full-width half-maximum (FWHM) Gaussian kernel. See supplementary materials for detailed *fMRIPrep* pre-processing pipeline. A generalized linear model was used to regress white matter and cerebrospinal fluid signals and 6 head motion parameters (3 translation and 3 rotational). The time series for each region of interest (ROI) was calculated as the first principal component of the voxels' activity within an 8 mm sphere for larger regions (i.e., MPFC and

PCC) and a 6 mm sphere for all other regions. Boundaries of the masks constrained the spheres that were centred on MNI coordinates listed below.

Structural MRI Pre-processing

T1 data for all three timepoints were processed using the Computational Anatomy Toolbox (CAT12)[58]. When multiple sessions were available, CAT12's longitudinal pipeline utilised subject-specific templates and minimized morphometric estimation bias across time points[57]. Pre-processing included spatially adaptive non-local means denoising (SANLM)[59], bias field correction, and segmentation into grey matter (GM) and white matter (WM) using unified segmentation[60]. Resulting tissue maps were normalized to MNI space using diffeomorphic anatomical registration (DARTEL)[61] and modulated to preserve absolute tissue volumes, accounting for inter-individual brain size differences[62]. Modulated GM maps were smoothed with a 6mm FWHM Gaussian kernel, in alignment with fMRI preprocessing. See supplementary material for quality assurance.

Region of Interest Selection

For resting-state fMRI data, ROIs were selected based on previous literature[4,9,63], which included the medial prefrontal cortex (MPFC [3,54,-2]), PCC [0,-52,26], bilateral hippocampi (left [-29,-18,-16], right [29,-18,-16]), bilateral caudate (left [-10,14,0], right [10,14,0]), and bilateral putamen (left [-28,2,0], right [-28,2,0]). Masks were chosen using the WFU PickAtlas[64] for the PCC, hippocampi, caudate, and putamen, and Stanford Willard Atlas[65] for the MPFC. Masks further constrained the sphere around the MNI centroid.

For voxel-based morphometry (VBM) and linear mixed model (LMM) analyses, analyses were constrained to core regions (MPFC, PCC and bilateral hippocampus and striatum), using the Tian 3T S1 atlas for striatum and hippocampi[66] and Schaefer's 17 network 100 parcellation atlas for MPFC and PCC[67,68].

Voxel-Based Morphometry

VBM was implemented using SPM12 and MarsBaR[69]. A flexible factorial design[70–72] specified subject as a random factor, with time and group as fixed factors, as well as time by group interaction, to characterize volumetric trajectories[58]. Covariates included total intracranial volume (TIV)—to account for measurement variability[60]—, HD-ISS, and mood medication use. ROI comparisons were conducted using f and t contrasts, and statistical significance ($p < 0.05$) was applied with False Discovery Rate (FDR) correction for multiple comparisons across ROIs[62].

Linear Mixed Models

Two linear mixed models (LLMs) examined depressive symptoms, using either HADS-D or BDI-II score. Fixed effects were history of depression, TIV-normalized ROI volumes (scaled by 100), mood medication use, and HD-ISS. Random intercepts accounted for the hierarchical structure of repeated measures nested within participants[73]. Intraclass correlation coefficients (ICC) quantified between-subject variability, substantiating the inclusion of subject-specific random effects.

Restricted maximum likelihood estimation (REML) was used to obtain unbiased variance estimates by accounting for fixed effects degrees of freedom[73]. This approach accurately captured between-subject variability given the model structure (11 fixed effects) and sample-to-parameter ratio (n-p =22.1)[74]. Linear and quadratic session effects were compared to examine changes in depression symptoms over time. Model selection involved likelihood ratio tests (maximum likelihood estimation for nested models), information criteria evaluation (AIC and BIC) with preference for parsimonious solutions[75], and marginal R^2 values quantified variance explained by fixed effects. Model assumptions were met and are reported in supplementary materials. Analyses were conducted in R version 4.1.3[76] using lme4[77] and lmerTest[77], with $p \leq 0.05$ considered statistically significant.

Spectral Dynamic Causal Modelling

spDCM employs a linear state-space model to fit the cross-spectral densities of observed BOLD signals[8]. At the first level, for each participant, fully connected DCM models without exogenous input (i.e., resting state) were specified using our 8 predefined ROIs. Models were subsequently estimated by fitting the DCM forward model (i.e., its parameters) to match the observed cross-spectral densities, yielding estimates of effective connectivity strength between ROI pairs and the corresponding parameter uncertainty.

The longitudinal analysis framework examined connectivity patterns baseline and 24-month follow-up, with two change analyses, one for HDGECS with a depression history and one for HDGECs with no depression history. This approach allowed investigation of connectivity changes associated with depression symptoms within depression subgroups. Covariates included mood medication use and HD-ISS stage to control for confounding effects that varied across timepoints within HDGECs.

The inferred effective connectivity from the first-level analysis was used for hypothesis testing of effects of time within group (i.e., effective connectivity of 8 ROIs at 24-months with reference to baseline connectivity). The Parametric Empirical Bayes (PEB) framework was used to estimate the effect of a history of depression and time for each connection [37]. PEB incorporated both the expected connectivity strength and variance while accounting for between-subject variability and noise. Lastly, Bayesian model reduction (BMR) was employed as an efficient form of Bayesian model selection [37]. We focused on connections with free energy $\geq$ 0.95, amounting to strong evidence. Only connections exceeding this threshold are reported throughout. Self-connections, which modulate excitation-inhibition through synaptic decay regulation[36], were analysed alongside inter-regional connectivity parameters. More information is in Supplementary Material.

Data availability

No new data were collected for this article. The data that support the findings of this study are available on the Enroll-HD platform via request at https://www.enroll-hd.org/for-researchers/access-data-biosamples/.

Results

Participant Characteristics

Overall, 105 unique HDGECs were included across analyses. Due to data requirement differences across our VBM, LMM and DCM analyses, as well as quality control for structural and fMRI data, analyses included different participant subsets (Table 1).

Table 1 Sample Allocation Across Study Analyses

Analysis	Total *N*	No Depression History	Depression History	Total Observations	Requirements
Total	105	75	30	263	-
Voxel-Based Morphometry	71	53	18	142	Baseline and 24-month structural MRI; IQR >70%; passed manual QC
Linear Mixed Model	87	61	26	243	Minimum 2 sessions; complete BDI-II/HADS-D; demographic covariates
Spectral Dynamic Causal Modelling	102	71	31	164	Baseline OR 24-month fMRI; framewise displacement <0.5mm; <20% bad volumes

Sample size variations reflect different data requirements and quality control standards specific to each analysis method. IQR = Image Quality Rating; TIV = Total Intracranial Volume; QC = Quality Control; obs = observations.

For example, for analyses of brain changes (both volumetry and effective connectivity), we used baseline and 24-month follow-up data to capture meaningful brain changes, as cortical atrophy is more subtle in HDGECs[10,46,78]. At each participant's first available session, those with a history of depression had significantly higher rates of mood medication use. No other variables differed significantly (Table 2).

Table 2 Demographic, Clinical, and Psychiatric Characteristics of HDGECs

	No History of Depression (*N* = 75)	History of Depression (*N* = 30)	*p* value
Demographic Variables			
Age			.983[b]
Mean (SD)	43 (9.91)	43.1 (7.43)	
Range	23.00 - 68.00	28.00 - 60.00	
Sex			.422[a]
Female	36 (48.00%)	17 (56.67%)	
Male	39 (52.00%)	13 (43.33%)	
Ethnicity			.646[a]
White	71 (94.67%)	29 (96.67%)	
American - Latin	1 (1.33%)	1 (3.33%)	
Asian - East	2 (2.67%)	0 (0.00%)	
Mixed	1 (1.33%)	0 (0.00%)	
Handedness			.397[a]
Right-handed	69 (92.00%)	25 (83.33%)	
Left-handed	3 (4.00%)	3 (10.00%)	

Ambidextrous	3 (4.00%)	2 (6.67%)	
HD-related Variables			
CAG Repeat Length			.963[b]
Mean (SD)	43.32 (2.38)	43.1 (1.81)	
Range	40.00 - 49.00	39.00 - 47.00	
DBS Score			.322[b]
Mean (SD)	305.02 (52.68)	314.18 (55.36)	
Range	185.00 - 443.00	179.00 - 401.00	
HD-ISS Stage			.476[a]
0	23 (30.67%)	6 (20.00%)	
1	30 (40.00%)	14 (46.67%)	
2	19 (25.33%)	7 (23.33%)	
3	3 (4.00%)	3 (10.00%)	
Depression Variables			
Current Depression			< .001[a]
No Current Depression	75 (100.00%)	14 (46.67%)	
Current Depression	0 (0.00%)	16 (53.33%)	
BDI-II Score			.174[b]
Mean (SD)	6.01 (7.27)	8.93 (11.1)	
Range	0.00 - 27.00	0.00 - 46.00	
HADS-D Score			.063[b]
Mean (SD)	2.60 (3.47)	4.33 (5.2)	
Range	0.00 - 14.00	0.00 - 19.00	
BDI-II Clinical Cut-off			.664[a]
Clinically Sig. Symptoms	17 (22.67%)	8 (26.67%)	
Low Depressive Symptoms	58 (77.33%)	22 (73.33%)	
HADS-D Clinical Cut-off			.391[a]
Clinically Sig. Symptoms	10 (13.33%)	6 (20.00%)	
Low Depressive Symptoms	65 (86.67%)	24 (80.00%)	
Suicidal Ideation History			.073[a]
No	62 (82.67%)	20 (66.67%)	
Yes	13 (17.33%)	10 (33.33%)	
Suicide Attempt History			.231[a]
No	72 (96.00%)	27 (90.00%)	
Yes	3 (4.00%)	3 (10.00%)	
Mood Medication Use			< .001[a]
No	15 (45.45%)	60 (83.33%)	
Yes	18 (54.55%)	12 (16.67%)	
Session Completed			
Visit 1 Only	10 (13.33%)	7 (23.33%)	
Visits 1 & 2 Only	10 (13.33%)	5 (16.67%)	
Visits 1 & 3 Only	3 (4.00%)	2 (6.67%)	
Visits 2 & 3 Only	1 (1.33%)	1 (3.33%)	
All Three Sessions	51 (68.00%)	15 (50.00%)	

SD = standard deviation. CAG = cytosine-adenine-guanine. CAP = CAG-Age Product. DBS = Disease Burden Score. BDI-II = the Beck Depression Inventory, 2nd Edition. HADS-D = the Hospital Anxiety and Depression Scale, Depression Subscale.
[a]Pearson's Chi-squared test
[b]Linear ANOVA

Voxel-Based Morphometry Results

VBM included 71 HDGECs, totalling 142 sessions, using both baseline and 24-month follow-up. There were 18 HDGECs with a history of depression and 53 HDGECs without a history of

depression. Further details in Supplementary Results. Patterns of grey matter volume reductions were compared for HDGECs with and without depression history over 24 months (Table 3).

Table 3 Grey Matter Volume Changes Over 24 Months

	Overall Model		Overall Effect of Time		Non-Depression Group		Depression Group		Group × Time Interaction	
Region	**F**	**p_{corr}**	**t**	**p_{corr}**	**t**	**p_{corr}**	**t**	**p_{corr}**	**t**	**p_{corr}**
CAU_R	16.09	**< .001**	4.34	**< .001**	4.11	**< .001**	3.17	**< .001**	0.26	.983
CAU_L	54.68	**< .001**	7.85	**< .001**	8.90	**< .001**	4.71	**< .001**	-1.56	1.000
PU_R	16.69	**< .001**	4.30	**< .001**	5.65	**< .001**	2.03	.172	-1.94	1.000
PU_L	31.95	**< .001**	6.97	**< .001**	7.20	**< .001**	4.67	**< .001**	-0.42	1.000
HPC_R	6.79	**< .001**	0.24	1.000	0.77	.937	-0.21	.985	-0.74	1.000
HPC_L	7.94	**< .001**	2.19	.164	2.04	.181	1.63	.232	0.18	.989
PCC	24.78	**< .001**	-1.06	.946	-1.13	1.000	-0.69	1.000	0.11	.992
MPFC	14.18	**< .001**	0.30	1.000	1.50	.327	-0.63	1.000	-1.66	1.000

p_{corr} *=p-values FWE-corrected at the ROI level. Group × Time Interaction tests whether volumetric changes from Time 1 to Time 2 were more pronounced in HDGECs depression history*. MPFC = Medial Prefrontal Cortex; PCC = Posterior Cingulate Cortex; HPC_L = Left Hippocampus; HPC_R = Right Hippocampus; CAU_L = Left Caudate; PU_L = Left Putamen; PU_R = Right Putamen.

When looking at all HDGECs and for HDGECs with no history of depression, all striatal regions exhibited significant volume loss, however, there was more selective striatal volume loss in HDGECs with a history of depression, with no significant reduction in right putamen grey matter. No DMN regions showed significant volume changes over 24 months in either group. Group by time interactions revealed no differential atrophy patterns between depression and non-depression groups across any examined region.

Linear Mixed Model of Depression Symptoms

LMMs included 87 HDGECs, using all three timepoints. There were 26 HDGECs with a history of depression (73% all three sessions) and 61 HDGECs without a history of depression (82% all three sessions). Further details in Supplementary Results. LLMs with linear time trajectories demonstrated optimal fit across both models (see Supplementary Results). There was substantial between-subject heterogeneity and ICC indicated individual differences accounted for 73.2% and 68.5% of total variance in HADS-D and BDI-II scores, respectively. Variance explained by fixed effects alone was modest (marginal R^2: HADS-D = 0.119; BDI-II = 0.072), with random intercepts increasing explanatory power (conditional R^2: HADS-D = 0.764; BDI-II = 0.708). Fig.

1A shows the results as a forest plot of standardized β coefficients and 95% confidence intervals (detailed in Supplementary Table 5).

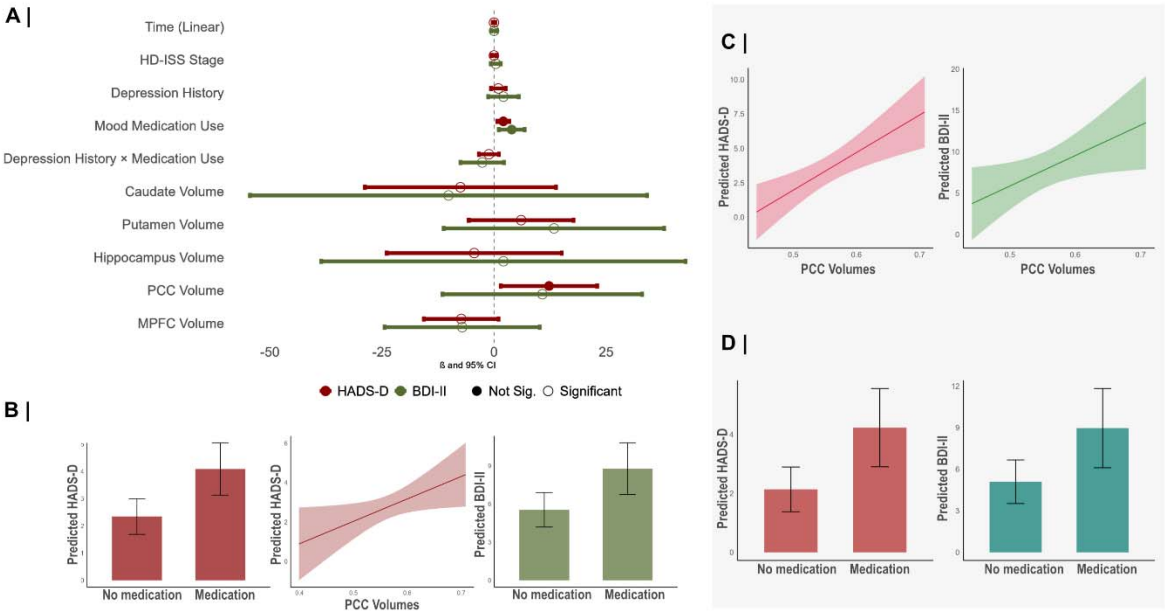

Fig. 1 Predictors of Depression Symptoms at 24-month Follow-up. (A) Forest plot displaying standardized β coefficients and 95% confidence intervals from linear mixed-effects models predicting Beck Depression Inventory-II (BDI-II; green) and Hospital Anxiety and Depression Scale-Depression subscale (HADS-D; red). Fixed effects include clinical variables (HD-ISS stage, depression history, antidepressant use). All brain volumes are normalized by total intracranial volume (TIV) and scaled (×100) (caudate, putamen, hippocampus, posterior cingulate cortex [PCC], medial prefrontal cortex [MPFC]). Filled circles indicate statistical significance. **(B)** Predicted BDI-II and HADS-D scores stratified by medication use and scatter plot illustrating the relationship between PCC volume and HADS-D scores with regression line and 95% confidence interval (shaded region). **(C)** Scatter plot illustrating the relationship between PCC volume and HADS-D and BDI-II scores with regression line and 95% confidence interval (shaded region), for HDGECs with a history of depression. **(D)** Predicted HADS-D and BDI-II scores stratified by medication class for HDGECs with no depression history.

Fixed Effects Predicting Depressive Symptoms

Mood medication use was associated with both elevated BDI-II (p = .008) and HADS-D scores (p = . 003; Fig. 1A). There was significant and overlapping variability in predicted scores (shown in error bars of Fig. 1B). Additionally, there was a positive association between PCC volumes and depression severity on the HADS-D (p = .03), with larger PCC volumes associated with increased depressive symptoms (Fig. 1B).

When analyses were constrained to HDGECs with a history of depression, larger PCC volumes were associated with more severe symptoms on both BDI-II, β = 36.79, SE = 16.88, t(19.70) = 2.18, p = .041, and HADS-D, β = 27.31, SE = 7.85, t(22.04) = 3.48, p = .002 (Fig. 1C), however,

for HDGECs with no history of depression, anti-depressant use was the only significant association for HADS-D, $\beta = 2.10$, $SE = 0.68$, $t(158.43) = 3.08$, $p = .002$, and BDI-II, $\beta = 3.86$, $SE = 1.49$, $t(150.87) = 2.60$, $p = .010$ (Fig. 1D). See Supplementary Fig. 9 and 10 for forest plots of standardized β coefficients.

Effective Connectivity Changes

DMN and Striatal Effective Connectivity Changes over 24-months for HDGECS with and Without Depression History

The analyses included 102 HDGECs, using baseline and 24-month follow-up data. There were 31 HDGECs with a history of depression (51% both sessions) and 71 HDGECs with no history of depression (64.8% both sessions). Further details in Supplementary Results. The estimation of DCM models for HDGECs with a history of depression was excellent, with mean variance explained by the model of 88.6% (*SD* = 4.5, 74.12-94.31; baseline = 88.5%, 24-month follow-up = 88.7%). Results were similar for HDGECs with no history of depression, with mean variance explained by the model of 90.4% (*SD* = 3.8, 75.15-96.45; baseline = 90.5%, 24-month follow-up = 90.3%).

Fig. 2 presents the effective connectivity changes observed across HDGECs stratified by depression history over the 24-month period. The two spDCM analyses identified three distinct connectivity profiles: depression history specific alterations (Fig 2A), shared connectivity changes (Fig. 2B), and no depression history specific modifications (Fig. 2C). Shared connectivity changes were effective connections that had the same valence (inhibition or excitation) and direction of change (increased or decreased connectivity) across both analyses.

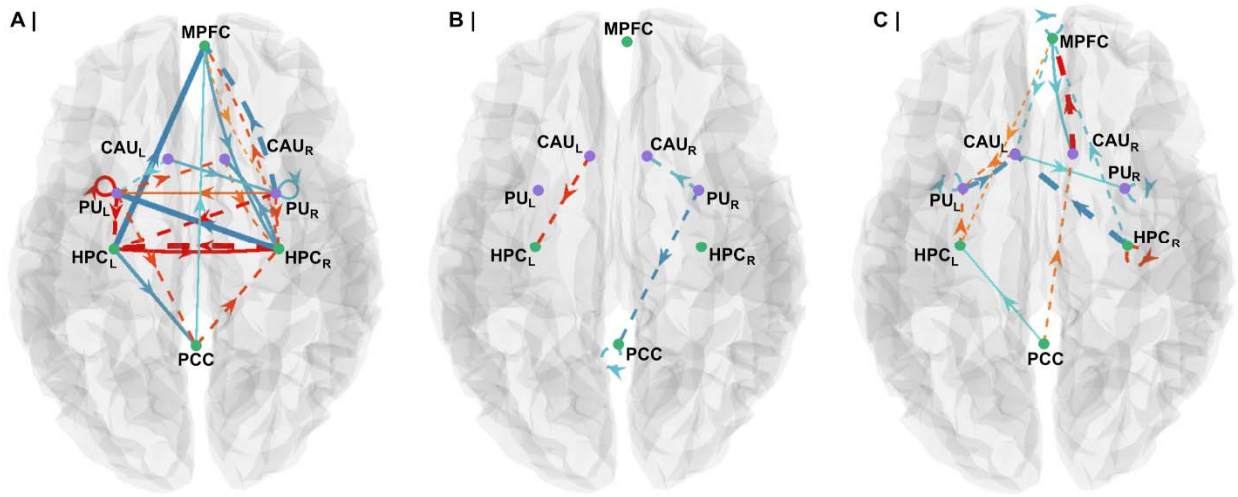

Fig. 2 Differences and Similarities in Effective Connectivity Changes for HDGECs with and without a History of Depression over 24 Months compared to baseline. **(A)** shows the unique effective connectivity changes for HDGECs with a history of depression, with connection strength represented by edge width. **(B)** shows effective connections that have the same pattern of change for both groups across 24 months. **(C)** shows effective connection changes over 24 months that are unique to the no-history of depression group, with connection strength represented by edge width. DMN nodes are shown in green and striatal nodes in purple. Increased connectivity in yellow-red and decreased connectivity in aqua-navy. Solid lines represent excitatory connections, dashed inhibitory. MPFC = Medial Prefrontal Cortex; PCC = Posterior Cingulate Cortex; HPC_L = Left Hippocampus; HPC_R = Right Hippocampus; CAU_L = Left Caudate; CAU_R = Left Caudate; PU_L = Left Putamen; PU_R = Right Putamen.

Posterior expectation and connection strength differed for shared connections and are reported in Table 4, alongside between-region effective connectivity changes, including valences, posterior expectations and credible intervals.

Effective Connectivity Changes and Depressive Symptoms

There were no significant differences in depression symptoms between baseline and 24 months for either BDI-II, $t(60) = -0.074$, $p = 0.94$, or HADS-D, $t(60) = 0.057$, $p = 0.95$. Therefore, we used significant connections for each group to see if the change in connectivity over 24 months was associated with clinically elevated depression symptoms at 24-month follow-up, for HDGECs with a history of depression (Fig. 3) and those without (Fig. 4).

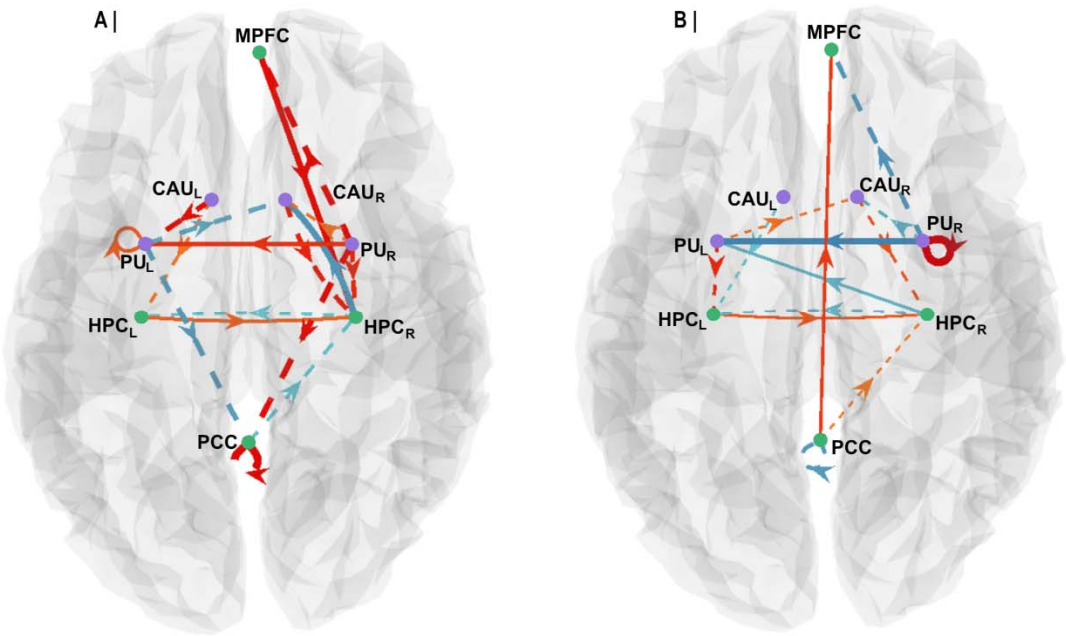

Fig. 3 Effective Connectivity Changes for HDGECs with a History of Depression Associated with Clinically Elevated Depressive Symptoms. (A) Regional connectivity changes associated with clinical cut-off for BDI-II. **(B)** Regional connectivity changes associated with meeting cut-off for HADS-D. **(C)** The arrows show the directed influence of one region on another, including self-connections. Increased connectivity in yellow-red and decreased connectivity in aqua-navy, , with connection strength represented by edge width. Solid lines represent excitatory connections, dashed inhibitory. MPFC = Medial Prefrontal Cortex; PCC = Posterior Cingulate Cortex; HPC$_L$ = Left Hippocampus; HPC$_R$ = Right Hippocampus; CAU$_L$ = Left Caudate; CAU$_R$ = Left Caudate; PU$_L$ = Left Putamen; PU$_R$ = Right Putamen.

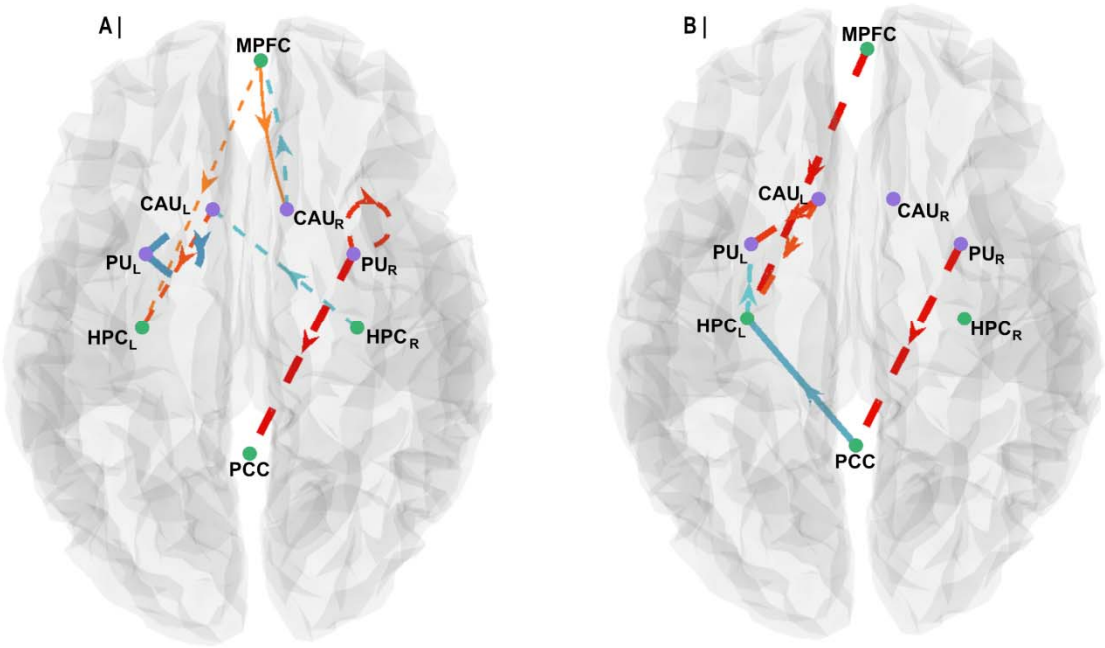

Fig. 4 Effective Connectivity Changes for HDGECs with no History of Depression Associated with Clinically Elevated Depressive Symptoms. (A) Regional connectivity changes associated with clinical cut-off for BDI-II. **(B)** Regional connectivity changes associated with meeting cut-off for HADS-D. **(C)** The arrows show the directed influence of one region on another, including self-connections. Solid lines represent increased connectivity while dashes represent decreased connectivity. Increased connectivity in yellow-red and decreased connectivity in aqua-navy, , with connection strength represented by edge width. Solid lines represent excitatory connections, dashed inhibitory. MPFC = Medial Prefrontal Cortex; PCC = Posterior Cingulate Cortex; HPC_L = Left Hippocampus; HPC_R = Right Hippocampus; CAU_L = Left Caudate; CAU_R = Left Caudate; PU_L = Left Putamen; PU_R = Right Putamen.

Discussion

Depression in HDGECs can be understood as a network dysconnection syndrome, arising from connectivity changes in large-scale functional brain networks[79]. Here we show that changes in effective connectivity of DMN and striatum differentiate HDGECs with a history of depression from those without. Moreover, these changes occur in the absence of differentiating patterns of grey matter atrophy in any region. Larger PCC volumes correlated with increased depression severity—specifically in HDGECs with history of depression—contradicting the classical neuroscientific view linking structural preservation to reduced vulnerability. Instead, our findings contribute to a growing literature that suggests functional rearrangement and pathological processes of relatively preserved regions in networks underpins some signs and symptoms in HD.

Grey Matter Atrophy Does Not Differentiate HDGECs with Depression

VBM analyses showed striatal degeneration across all HDGECs, with no difference in atrophy patterns across striatal and cortical regions over 24 months. HD is characterized by early and severe striatal atrophy—comprising caudate and putamen—including in HDGECs[14–16], and our findings align with early and frank atrophy of grey matter in the striatum. Major depression has been associated with grey matter atrophy in dorsolateral and dorsomedial prefrontal cortices and posterior cingulate when compared to non-depressed controls[80]. Our findings failed to find similar patterns when compared to non-depressed HDGECs. It's possible that regional volume differences may occur when compared to non-HD controls, that are missed by looking at brain change over 24 months only within HDGECs. Following the same cohort as the current study

over 10 years, HDGECs have shown pronounced striatal and posterior driven (from occipital pole forwards) atrophy trajectories in the long-term transition to manifest HD, when compared to age-matched controls[15]. Johnson et al. (2021) did not include hippocampus, prefrontal cortices, and included a composite of the cingulate gyrus (including PCC), and their results focussed on cognitive and motor correlates of brain atrophy. It's possible that similar patterns of atrophy trajectories may appear over longer time periods, including the transition to manifest HD, in our depression-related regions. To further explore this relationship, analyses comparing depression in HDGECs with both non-depression controls and idiopathic major depression would elucidate whether brain atrophy follows similar or divergent patterns over disease progression.

Additionally, we failed to find an association between increased atrophy and depressive symptoms over 24-months. Our study finding aligns with existing research that found no correlation between striatal atrophy and depressive symptoms in HDGECs[32], and extends this to include depression-related regions. Instead, our findings show larger PCC volumes associated with more severe depression symptoms for the HADS-D, regardless of depression history. Critically, when we looked at HDGECs with a history of depression, we saw that this relationship extended to the BDI-II, however, associations were lost for HDGECs without a history of depression. This suggests an alteration in the structure-function relationship in HDGECs with a comorbid depression history, and may represent functional reorganisation unique to depression in HD. Broadly, the PCC has been proposed as a disease epicenter for HDGECs, with significant structural connectivity reductions[21] and in major depression, more severe depressive mood has been associated with larger PCC volumes in older adults with subthreshold depressive symptoms[81]. The disease process for HDGECs may increase risk for more severe depressive symptoms, and links disparate threads to suggest PCC functional reorganisation as a HDGEC depression-specific mechanism. Previous findings, based on a single question regarding low mood, found reduced cortical thickness in DMN regions (left ventromedial prefrontal cortex, medial temporal gyrus, PCC), as well as reduced grey matter in ventromedial prefrontal cortex and middle temporal gyri, with concurrent increased grey matter in right caudate[5]. One key limitation of this research is that it collapses HDGECs with manifest HD, making it difficult to tease apart the asynchronous and asymmetric pattern of both neurodegeneration and depression in HD. Our findings help elucidate that these patterns of grey matter reductions may be driven by changes in later HD periods, suggesting compensatory

structural alterations precede atrophic patterns observed in later disease stages. This temporal sequence suggests a biphasic model of depression-related structural changes in HD: initial compensatory mechanisms in key network hubs during early premanifest stages, followed by progressive atrophic patterns as disease advances. The transition from our findings of increased PCC volume to Garcia-Gorro et al.'s (2019) documented PCC reductions may represent disease stage specific changes, wherein initially adaptive compensatory structural responses due to relative preservation of cortical regions become maladaptive as neurodegenerative processes overwhelm compensatory mechanisms.

Effective Connectivity Changes of Depression for HDGECs

The longitudinal connectivity patterns extend our previous cross-sectional findings[4] while revealing the temporal evolution of network dysfunction. For HDGECs with a history of depression, connectivity changes over 24-months were more widespread and interhemispheric generally. In keeping with previous findings in both major depression[34,35] and our cross-sectional work[4], there was a propensity for right hemispheric aberrations in effective connectivity. This is in contrast with previous work in HD showing leftward putamen grey matter loss associated with emotion processing[33], suggesting potential mechanisms of function-structure dissociation. Left putamen had decreasing inhibitory control on both right caudate and left hippocampus, however, effective connectivity patterns show bilateral putamen involvement in depression trajectories. When we look at specific patterns, there is dissociable disinhibition of MPFC on right putamen and conversely increasing inhibitory control of right putamen on MPFC. In previous cross-sectional work, right putamen had reduced inhibitory control over MPFC[4], and this appears to become increasingly inhibitory over 24-months. In terms of hippocampal connectivity, left hippocampus has inhibitory influence on both hubs of the DMN, while right hippocampus has reduced excitatory influence on the striatum. Cross-sectional work showed right hippocampus inhibitory control over left caudate[4], suggesting dynamic alterations in effective connectivity over disease progression in line with comorbid depression for HDGECs. These longitudinal connectivity patterns extend our previous cross-sectional findings[4] while revealing the temporal evolution of network dysfunction.

Changes in effective connectivity of HDGECs without depression provide insight into connectivity processes related to HD pathogenesis. We found evidence of aberrant MPFC control over bilateral caudate, that is increasingly inhibitory in left hemisphere and hypoexcitatory in the right. Additionally, HD progression is associated with aberrant self-connectivity of MPFC, suggesting accelerated synaptic decay. Right hippocampus inhibition is influential in HD pathogenesis with reduced synaptic decay (disinhibition) and hypoexcitation with left caudate. Interestingly, we saw that at baseline, increasing inhibition of right hippocampus to right caudate differentiate HDGECs with depression history from those without[4]. This suggests that as HD progresses, compensatory mechanisms of right hippocampus in those without depression may break down and become maladaptive as neurodegenerative burden increases. Some shared connections across groups showed opposite valences, with HDGECs with depression showing increased inhibitory control of right putamen to PCC, hypoexcitation of right putamen self-connectivity and hyperexcitation of left putamen self-connectivity over 24 months. By contrast, HDGECs with no depression history showed hypoexcitation of right putamen to PCC and accelerated synaptic decay of bilateral putamen. These findings suggest depression in HDGECs results in aberrant effective connectivity changes of our previously proposed epicenters for depression in premanifest HD[4].

Although there was heterogeneity across BDI-II and HADS-D, some effective connections differentiated HDGECs with depression and those without. For HDGECs with a history of depression, clinically elevated depressive symptoms were associated with reduced excitation of right to left hippocampus and disinhibition of both left hippocampus and right caudate to right hippocampus, when compared to those who did not meet the clinical cut-off for the BDI-II or HADS-D. PCC hyperconnectivity is associated with elevated depressive symptoms in PD[31], however, our findings show more complex patterns of aberrant inhibitory self-connectivity of PCC and PCC to right hippocampus. These changes are unique to HDGECs with a depression history, suggesting a potential joined mechanism across PD and HD of aberrant PCC connectivity associated with depression severity. By comparison, for HDGECs with no history of depression, clinically elevated depressive symptoms were associated with increased excitation of right putamen to PCC and disinhibition of both MPFC and left caudate to left hippocampus. These findings suggest HDGECs without depression history retain greater neural flexibility in managing mood-related dysfunction, whereas those with a history of depression may become

increasingly reliant on compromised striatal circuits, as well as HD-disease epicenters (putamen, PCC and hippocampus) to maintain emotional regulation. Such neural resource allocation may create a progressively maladaptive feedback loop in HDGECs with depression, where core HD pathology and depression become increasingly intertwined through shared network dysfunction.

Future Directions

Our sample comprised HDGECs in early stages of premanifest HD; with 73% of HDGECs falling in HD-ISS stage 0 or 1, representing minimal biological consequences of HD. Given that cortical volume changes appear to emerge during the transition period to clinical motor diagnosis[15], we may have missed the period of volumetric changes that would be associated with depression in HDGECs. A similar pattern of depression preceding structural atrophy is seen in PD depression where early depression severity predicted faster cortical thinning rates[29]. The findings of larger PCC volumes being associated with depression symptoms suggest we have captured a period of neural reorganisation. Moreover, volumetric changes represent only one dimension of structural brain organization and our analyses examined structure and function independently, rather than modelling the dynamic interactions of structural and effective connective coupling. Existing literature in HD has shown an inverse relationship between structural and functional connectivity, whereby stronger structural connectivity is associated with weaker functional activity—and vice versa—as well as dissociable patterns of network disruption affecting anterior and posterior brain systems[82]. This is yet to be explored in HDGECs or relation to depression. The mechanistic relationship between structural and functional connectivity—termed structure-function coupling (SFC)—has emerged to understand disease-related network reorganization[83]. A question arises whether neurodegeneration forces functional networks to collapse toward structural constraints, or HD pathogenesis engenders functional-structural decoupling through compensatory mechanisms.

Empirical research in Alzheimer's disease (AD) and major depression provides some preliminary evidence to support investigation of SFC in depression in HDGECs. Some suggest progressive structure-function decoupling across AD with mild cognitive impairment with intermediate coupling values[84], while others report increased SFC in the DMN in AD[85]—suggested to represent functional collapse to structure. This contradictory pattern suggests that

SFC is altered in neurodegeneration, but the pattern of alterations remains contentious. Major depression is associated with functional connectivity aberrations alongside intact structural networks, as well as interhemispheric decreased SFC that occurred alongside a positive association with depression symptom severity[86]. Decoupling may be a marker of network dysfunction in depression and aligns with our findings of preserved structure with aberrant effective connectivity. What remains unexplored is the interaction between the neurodegenerative process in HDGECs, which appears to result in potentially either decoupling or functional collapse, and depression, which appears to be characterized by functional reorganisation and decoupling. Given the focus on compensation as an explanatory mechanism for cognition[22,38] and now depression in HD, there remains an answered question about the critical period where structural-functional relationships may fundamentally reorganize. Using structurally informed priors for effective connectivity analyses is an emerging field, with growing interest[87]. Recent work has proposed a hierarchical empirical Bayes (HEB) model that leverages structural connectivity-based group level priors for DCM, enabling both between-group structure-function coupling comparisons and refined subject-level posterior estimates through a three-level Bayesian framework[88]. Investigating structure-function coupling dynamics in HD could elucidate whether observed network dysconnection patterns represent early functional alterations preceding structural breakdown or reflect compensatory responses to structural connectivity patterns not captured by volumetric measures.

Conclusion

Our findings suggests that depression for HDGECs emerges through network dysconnection that operates independently of regional atrophy. Functional alterations may precede detectable structural breakdown in the DMN and represent early compensatory or pathological responses to subclinical neurodegenerative processes.

Supplementary material

Supplementary material is available online.

References

1. Epping EA, Paulsen JS. Depression in the early stages of Huntington disease. *Neurodegener Dis Manag*. 2011;1(5):407-414. doi:10.2217/nmt.11.45

2. McAllister B, Gusella JF, Landwehrmeyer GB, et al. Timing and Impact of Psychiatric, Cognitive, and Motor Abnormalities in Huntington Disease. *Neurology*. 2021;96(19):e2395-e2406. doi:10.1212/WNL.0000000000011893

3. Pla P, Orvoen S, Saudou F, David DJ, Humbert S. Mood disorders in Huntington's disease: from behavior to cellular and molecular mechanisms. *Front Behav Neurosci*. 2014;8(135). Accessed March 10, 2022. https://doi.org/10.3389/fnbeh.2014.00135

4. Barta T, Novelli L, Georgiou-Karistianis N, et al. Depression in Premanifest Huntington's Disease: Aberrant Effective Connectivity of Striatum and Default Mode Network. Published online March 18, 2024. doi:10.1101/2024.03.17.24304066

5. Garcia-Gorro C, Llera A, Martinez-Horta S, et al. Specific patterns of brain alterations underlie distinct clinical profiles in Huntington's disease. *NeuroImage: Clinical*. 2019;23:101900. doi:10.1016/j.nicl.2019.101900

6. McColgan P, Razi A, Gregory S, et al. Structural and functional brain network correlates of depressive symptoms in premanifest Huntington's disease. *Human Brain Mapping*. 2017;38(6):2819-2829. doi:10.1002/hbm.23527

7. Friston KJ, Kahan J, Biswal B, Razi A. A DCM for resting state fMRI. *NeuroImage*. 2014;94:396-407. doi:10.1016/j.neuroimage.2013.12.009

8. Novelli L, Friston K, Razi A. Spectral dynamic causal modeling: A didactic introduction and its relationship with functional connectivity. *Network Neuroscience*. Published online January 19, 2024:1-25. doi:10.1162/netn_a_00348

9. Razi A, Kahan J, Rees G, Friston KJ. Construct validation of a DCM for resting state fMRI. *NeuroImage*. 2015;106:1-14. doi:10.1016/j.neuroimage.2014.11.027

10. Tabrizi SJ, Scahill RI, Owen G, et al. Predictors of phenotypic progression and disease onset in premanifest and early-stage Huntington's disease in the TRACK-HD study: analysis of 36-month observational data. *The Lancet Neurology*. 2013;12(7):637-649. doi:10.1016/S1474-4422(13)70088-7

11. Dale M, Maltby J, Shimozaki S, Cramp R, Rickards H. Disease stage, but not sex, predicts depression and psychological distress in Huntington's disease: A European population study. *Journal of Psychosomatic Research*. 2016;80:17-22. doi:10.1016/j.jpsychores.2015.11.003

12. Connors MH, Teixeira-Pinto A, Loy CT. Apathy and Depression in Huntington's Disease: Distinct Longitudinal Trajectories and Clinical Correlates. *JNP*. Published online September 21, 2022:appi.neuropsych.21070191. doi:10.1176/appi.neuropsych.21070191

13. Maltby J, Ovaska-Stafford N, Gunn S. The structure of mental health symptoms in Huntington's disease: Comparisons with healthy populations. *Journal of Clinical and Experimental Neuropsychology*. 2021;43(7):737-752. doi:10.1080/13803395.2021.2002824

14. Georgiou-Karistianis N, Gray MA, Domínguez D JF, et al. Automated differentiation of pre-diagnosis Huntington's disease from healthy control individuals based on quadratic discriminant analysis of the basal ganglia: The IMAGE-HD study. *Neurobiology of Disease*. 2013;51:82-92. doi:10.1016/j.nbd.2012.10.001

15. Johnson EB, Ziegler G, Penny W, et al. Dynamics of Cortical Degeneration Over a Decade in Huntington's Disease. *Biol Psychiatry*. 2021;89(8):807-816. doi:10.1016/j.biopsych.2020.11.009

16. Tabrizi SJ, Langbehn DR, Leavitt BR, et al. Biological and clinical manifestations of Huntington's disease in the longitudinal TRACK-HD study: cross-sectional analysis of baseline data. *The Lancet Neurology*. 2009;8(9):791-801. doi:10.1016/S1474-4422(09)70170-X

17. Bora E, Harrison BJ, Davey CG, Yücel M, Pantelis C. Meta-analysis of volumetric abnormalities in cortico-striatal-pallidal-thalamic circuits in major depressive disorder. *Psychological Medicine*. 2012;42(4):671-681. doi:10.1017/S0033291711001668

18. Lynch CJ, Elbau IG, Ng T, et al. Frontostriatal salience network expansion in individuals in depression. *Nature*. Published online September 4, 2024:1-10. doi:10.1038/s41586-024-07805-2

19. Meng C, Brandl F, Tahmasian M, et al. Aberrant topology of striatum's connectivity is associated with the number of episodes in depression. *Brain*. 2014;137(2):598-609. doi:10.1093/brain/awt290

20. Koval I, Dighiero-Brecht T, Tobin AJ, et al. Forecasting individual progression trajectories in Huntington disease enables more powered clinical trials. *Sci Rep*. 2022;12(1):18928. doi:10.1038/s41598-022-18848-8

21. Estevez-Fraga C, Sebenius I, Hansen JY, et al. Cell-specific mechanisms drive connectivity across the time course of Huntington's disease. *Nat Commun*. 2025;16(1):5519. doi:10.1038/s41467-025-60556-0

22. Gregory S, Long JD, Klöppel S, et al. Testing a longitudinal compensation model in premanifest Huntington's disease. *Brain*. 2018;141(7):2156-2166. doi:10.1093/brain/awy122

23. Li B, Liu L, Friston KJ, et al. A Treatment-Resistant Default Mode Subnetwork in Major Depression. *Biological Psychiatry*. 2013;74(1):48-54. doi:10.1016/j.biopsych.2012.11.007

24. Li B, Friston K, Mody M, Wang HN, Lu HB, Hu DW. A brain network model for depression: From symptom understanding to disease intervention. *CNS Neuroscience & Therapeutics*. 2018;24(11):1004-1019. doi:10.1111/cns.12998

25. Mulders PC, van Eijndhoven PF, Schene AH, Beckmann CF, Tendolkar I. Resting-state functional connectivity in major depressive disorder: A review. *Neuroscience & Biobehavioral Reviews*. 2015;56:330-344. doi:10.1016/j.neubiorev.2015.07.014

26. Li L, Li B, Bai Y, et al. Abnormal resting state effective connectivity within the default mode network in major depressive disorder: A spectral dynamic causal modeling study. *Brain and Behavior*. 2017;7(7):e00732. doi:10.1002/brb3.732

27. Leentjens AFG, Van den Akker M, Metsemakers JFM, Lousberg R, Verhey FRJ. Higher incidence of depression preceding the onset of Parkinson's disease: A register study. *Movement Disorders*. 2003;18(4):414-418. doi:10.1002/mds.10387

28. Shiba M, Bower JH, Maraganore DM, et al. Anxiety disorders and depressive disorders preceding Parkinson's disease: A case-control study. *Movement Disorders.* 2000;15(4):669-677. doi:10.1002/1531-8257(200007)15:4<669::AID-MDS1011>3.0.CO;2-5

29. Hanganu A, Bruneau MA, Degroot C, et al. Depressive symptoms in Parkinson's disease correlate with cortical atrophy over time. *Brain Cogn*. 2017;111:127-133. doi:10.1016/j.bandc.2016.11.001

30. Yuan J, Liu Y, Liao H, et al. Alterations in cortical volume and complexity in Parkinson's disease with depression. *CNS Neuroscience & Therapeutics*. 2024;30(2):e14582. doi:10.1111/cns.14582

31. Lou Y, Huang P, Li D, et al. Altered brain network centrality in depressed Parkinson's disease patients. *Movement Disorders.* 2015;30(13):1777-1784. doi:10.1002/mds.26321

32. Jurgens CK, van de Wiel L, van Es ACGM, et al. Basal ganglia volume and clinical correlates in 'preclinical' Huntington's disease. *J Neurol*. 2008;255(11):1785-1791. doi:10.1007/s00415-008-0050-4

33. Minkova L, Habich A, Peter J, Kaller CP, Eickhoff SB, Klöppel S. Gray matter asymmetries in aging and neurodegeneration: A review and meta-analysis. *Human Brain Mapping*. 2017;38(12):5890-5904. doi:10.1002/hbm.23772

34. Sambataro F, Wolf ND, Pennuto M, Vasic N, Wolf RC. Revisiting default mode network function in major depression: evidence for disrupted subsystem connectivity. *Psychological Medicine*. 2014;44(10):2041-2051. doi:10.1017/S0033291713002596

35. Wang Z, Yuan Y, Bai F, et al. Altered functional connectivity networks of hippocampal subregions in remitted late-onset depression: a longitudinal resting-state study. *Neurosci Bull*. 2015;31(1):13-21. doi:10.1007/s12264-014-1489-1

36. Friston KJ, Harrison L, Penny W. Dynamic causal modelling. *NeuroImage*. 2003;19(4):1273-1302. doi:10.1016/S1053-8119(03)00202-7

37. Friston KJ, Litvak V, Oswal A, et al. Bayesian model reduction and empirical Bayes for group (DCM) studies. *NeuroImage*. 2016;128:413-431. doi:10.1016/j.neuroimage.2015.11.015

38. Klöppel S, Gregory S, Scheller E, et al. Compensation in Preclinical Huntington's Disease: Evidence From the Track-On HD Study. *EBioMedicine*. 2015;2(10):1420-1429. doi:10.1016/j.ebiom.2015.08.002

39. Huntington Study Group (Kieburtz K, primary author). The Unified Huntington's Disease Rating Scale: Reliability and Consistency. *Movement Disorders*. 1996;11(2):136-142. doi:10.1002/mds.870110204

40. Warner JH, Long JD, Mills JA, et al. Standardizing the CAP Score in Huntington's Disease by Predicting Age-at-Onset. *Journal of Huntington's Disease*. 2022;11(2):153-171. doi:10.3233/JHD-210475

41. Langbehn DR, Hayden MR, Paulsen JS, and the PREDICT-HD Investigators of the Huntington Study Group. CAG-repeat length and the age of onset in Huntington disease (HD): a review and validation study of statistical approaches. *Am J Med Genet B Neuropsychiatr Genet*. 2010;153B(2):397-408. doi:10.1002/ajmg.b.30992

42. Penney JB, Vonsattel JP, MacDonald ME, Gusella JF, Myers RH. CAG repeat number governs the development rate of pathology in Huntington's disease. *Annals of Neurology*. 1997;41(5):689-692. doi:10.1002/ana.410410521

43. Zhang Y, Long JD, Mills JA, et al. Indexing disease progression at study entry with individuals at-risk for Huntington disease. *American Journal of Medical Genetics Part B: Neuropsychiatric Genetics*. 2011;156(7):751-763. doi:10.1002/ajmg.b.31232

44. Lahr J, Minkova L, Tabrizi SJ, et al. Working Memory-Related Effective Connectivity in Huntington's Disease Patients. *Front Neurol*. 2018;9. doi:10.3389/fneur.2018.00370

45. Odish OFF, van den Berg-Huysmans AA, van den Bogaard SJA, et al. Longitudinal resting state fMRI analysis in healthy controls and premanifest Huntington's disease gene carriers: A three-year follow-up study. *Human Brain Mapping*. 2015;36(1):110-119. doi:10.1002/hbm.22616

46. Tabrizi SJ, Scahill RI, Durr A, et al. Biological and clinical changes in premanifest and early stage Huntington's disease in the TRACK-HD study: the 12-month longitudinal analysis. *The Lancet Neurology*. 2011;10(1):31-42. doi:10.1016/S1474-4422(10)70276-3

47. Tabrizi SJ, Reilmann R, Roos RA, et al. Potential endpoints for clinical trials in premanifest and early Huntington's disease in the TRACK-HD study: analysis of 24 month observational data. *The Lancet Neurology*. 2012;11(1):42-53. doi:10.1016/S1474-4422(11)70263-0

48. Tabrizi SJ, Schobel S, Gantman EC, et al. A biological classification of Huntington's disease: the Integrated Staging System. *Lancet Neurol*. 2022;21(7):632-644. doi:10.1016/S1474-4422(22)00120-X

49. Considine CM, Rossetti MA, Del Bene VA, et al. Huntington Study Group's Neuropsychology Working Group: Implementing Non-Motor Diagnostic Criteria. *Movement Disorders Clinical Practice*. 2023;10(12):1714-1724. doi:10.1002/mdc3.13910

50. Beck AT, Steer RA, Brown GK, others. Manual for the Beck depression inventory-II. *San Antonio, TX: Psychological Corporation*. 1996;1(82):10-1037.

51. Zigmond AS, Snaith RP. The hospital anxiety and depression scale. *Acta psychiatrica scandinavica*. 1983;67(6):361-370.

52. Mestre TA, van Duijn E, Davis AM, et al. Rating scales for behavioral symptoms in Huntington's disease: Critique and recommendations. *Movement Disorders*. 2016;31(10):1466-1478. doi:10.1002/mds.26675

53. De Souza J, Jones LA, Rickards H. Validation of self-report depression rating scales in Huntington's disease. *Movement Disorders*. 2010;25(1):91-96. doi:10.1002/mds.22837

54. Esteban O, Markiewicz CJ, Blair RW, et al. fMRIPrep: a robust preprocessing pipeline for functional MRI. *Nat Methods*. 2019;16(1):111-116. doi:10.1038/s41592-018-0235-4

55. Esteban O, Ciric R, Finc K, et al. Analysis of task-based functional MRI data preprocessed with fMRIPrep. *Nat Protoc*. 2020;15(7):2186-2202. doi:10.1038/s41596-020-0327-3

56. Esteban O, Birman D, Schaer M, Koyejo OO, Poldrack RA, Gorgolewski KJ. MRIQC: Advancing the automatic prediction of image quality in MRI from unseen sites. *PLOS ONE*. 2017;12(9):e0184661. doi:10.1371/journal.pone.0184661

57. Reuter M, Schmansky NJ, Rosas HD, Fischl B. Within-subject template estimation for unbiased longitudinal image analysis. *Neuroimage*. 2012;61(4):1402-1418. doi:10.1016/j.neuroimage.2012.02.084

58. Gaser C, Dahnke R, Thompson PM, Kurth F, Luders E, the Alzheimer's Disease Neuroimaging Initiative. CAT: a computational anatomy toolbox for the analysis of structural MRI data. *GigaScience*. 2024;13:giae049. doi:10.1093/gigascience/giae049

59. Manjón JV, Coupé P, Martí□Bonmatí L, Collins DL, Robles M. Adaptive non□local means denoising of MR images with spatially varying noise levels. *Magnetic Resonance Imaging*. 2010;31(1):192-203. doi:10.1002/jmri.22003

60. Ashburner J, Friston KJ. Unified segmentation. *NeuroImage*. 2005;26(3):839-851. doi:10.1016/j.neuroimage.2005.02.018

61. Ashburner J, Friston KJ. Diffeomorphic registration using geodesic shooting and Gauss–Newton optimisation. *NeuroImage*. 2011;55(3):954-967. doi:10.1016/j.neuroimage.2010.12.049

62. Dahnke R, Yotter RA, Gaser C. Cortical thickness and central surface estimation. *Neuroimage*. 2013;65:336-348. doi:10.1016/j.neuroimage.2012.09.050

63. Di X, Biswal BB. Identifying the default mode network structure using dynamic causal modeling on resting-state functional magnetic resonance imaging. *NeuroImage*. 2014;86:53-59. doi:10.1016/j.neuroimage.2013.07.071

64. Maldjian J, Laurienti P, Kraft R, Burdette J. An automated method for neuroanatomic and cytoarchitectonic atlas-based interrogation of fMRI data sets. *Neuroimage*. Published online July 25, 2003.

65. Altmann A, Ng B, Landau SM, Jagust WJ, Greicius MD. Regional brain hypometabolism is unrelated to regional amyloid plaque burden. *Brain*. 2015;138(12):3734-3746. doi:10.1093/brain/awv278

66. Tian Y, Margulies DS, Breakspear M, Zalesky A. Topographic organization of the human subcortex unveiled with functional connectivity gradients. *Nat Neurosci*. 2020;23(11):1421-1432. doi:10.1038/s41593-020-00711-6

67. Schaefer A, Kong R, Gordon EM, et al. Local-Global Parcellation of the Human Cerebral Cortex from Intrinsic Functional Connectivity MRI. *Cerebral Cortex*. 2018;28(9):3095-3114. doi:10.1093/cercor/bhx179

68. Thomas Yeo BT, Krienen FM, Sepulcre J, et al. The organization of the human cerebral cortex estimated by intrinsic functional connectivity. *Journal of Neurophysiology*. 2011;106(3):1125-1165. doi:10.1152/jn.00338.2011

69. Brett M, Anton JL, Valabregue R, Poline JB. Region of interest analysis using an SPM toolbox. Published online 2002.

70. Penny W, Friston K, Ashburner J, Kiebel S, Nichols T, eds. *Statistical Parametric Mapping: The Analysis of Functional Brain Images*. 1st Edition. Academic Press; 2006.

71. Kiebel SJ, Kherif AP, Holmes C. The General Linear Model. In: *Statistical Parametric Mapping*. ; 2007:101-125.

72. Poline JB, Kherif F, Pallier C, Penny W. Contrasts and Classical Inference. In: *Statistical Parametric Mapping*. ; 2007:126-139.

73. Tabachnick BG, Fidell LS. Multilevel Linear Modeling. In: *Using Multivariate Statistics*. Seventh edition. Always learning. Pearson; 2019:613-671.

74. Molenberghs G, Verbeke G, eds. Estimation of the Marginal Model. In: *Linear Mixed Models for Longitudinal Data*. Springer New York; 2000:41-54. doi:10.1007/978-1-4419-0300-6_5

75. Burnham KP, Anderson DR. Multimodel inference: understanding AIC and BIC in model selection. *Sociological methods & research*. 2004;33(2):261-304.

76. R Core Team. *R: A Language and Environment for Statistical Computing*. R Foundation for Statistical Computing; 2022. https://www.R-project.org/

77. Kuznetsova A, Brockhoff PB, Christensen RHB. lmerTest Package: Tests in Linear Mixed Effects Models. *J Stat Soft*. 2017;82(13):1-26. doi:10.18637/jss.v082.i13

78. Rosas HD, Liu AK, Hersch S, et al. Regional and progressive thinning of the cortical ribbon in Huntington's disease. *Neurology*. 2002;58(5):695-701. doi:10.1212/WNL.58.5.695

79. Hannan AJ. Synaptopathy, circuitopathy and the computational biology of Huntington's disease. *BMC Biology*. 2018;16(1):71. doi:10.1186/s12915-018-0539-y

80. Grieve SM, Korgaonkar MS, Koslow SH, Gordon E, Williams LM. Widespread reductions in gray matter volume in depression. *NeuroImage: Clinical*. 2013;3:332-339. doi:10.1016/j.nicl.2013.08.016

81. McLaren ME, Szymkowicz SM, O'Shea A, Woods AJ, Anton SD, Dotson VM. Dimensions of depressive symptoms and cingulate volumes in older adults. *Transl Psychiatry*. 2016;6(4):e788. doi:10.1038/tp.2016.49

82. McColgan P, Gregory S, Razi A, et al. White matter predicts functional connectivity in premanifest Huntington's disease. *Annals of Clinical and Translational Neurology*. 2017;4(2):106-118. doi:10.1002/acn3.384

83. Fotiadis P, Parkes L, Davis KA, Satterthwaite TD, Shinohara RT, Bassett DS. Structure–function coupling in macroscale human brain networks. *Nat Rev Neurosci*. 2024;25(10):688-704. doi:10.1038/s41583-024-00846-6

84. Sun Y, Yin Q, Fang R, et al. Disrupted Functional Brain Connectivity and Its Association to Structural Connectivity in Amnestic Mild Cognitive Impairment and Alzheimer's Disease. Tian J, ed. *PLoS ONE*. 2014;9(5):e96505. doi:10.1371/journal.pone.0096505

85. Dai Z, Lin Q, Li T, et al. Disrupted structural and functional brain networks in Alzheimer's disease. *Neurobiology of Aging*. 2019;75:71-82. doi:10.1016/j.neurobiolaging.2018.11.005

86. Jiang X, Shen Y, Yao J, et al. Connectome analysis of functional and structural hemispheric brain networks in major depressive disorder. *Transl Psychiatry*. 2019;9(1):136. doi:10.1038/s41398-019-0467-9

87. Greaves MD, Novelli L, Mansour L. S, Zalesky A, Razi A. Structurally informed models of directed brain connectivity. *Nat Rev Neurosci*. 2025;26(1):23-41. doi:10.1038/s41583-024-00881-3

88. Greaves MD, Novelli L, Razi A. Structurally informed resting-state effective connectivity recapitulates cortical hierarchy. Published online February 28, 2025:2024.04.03.587831. doi:10.1101/2024.04.03.587831

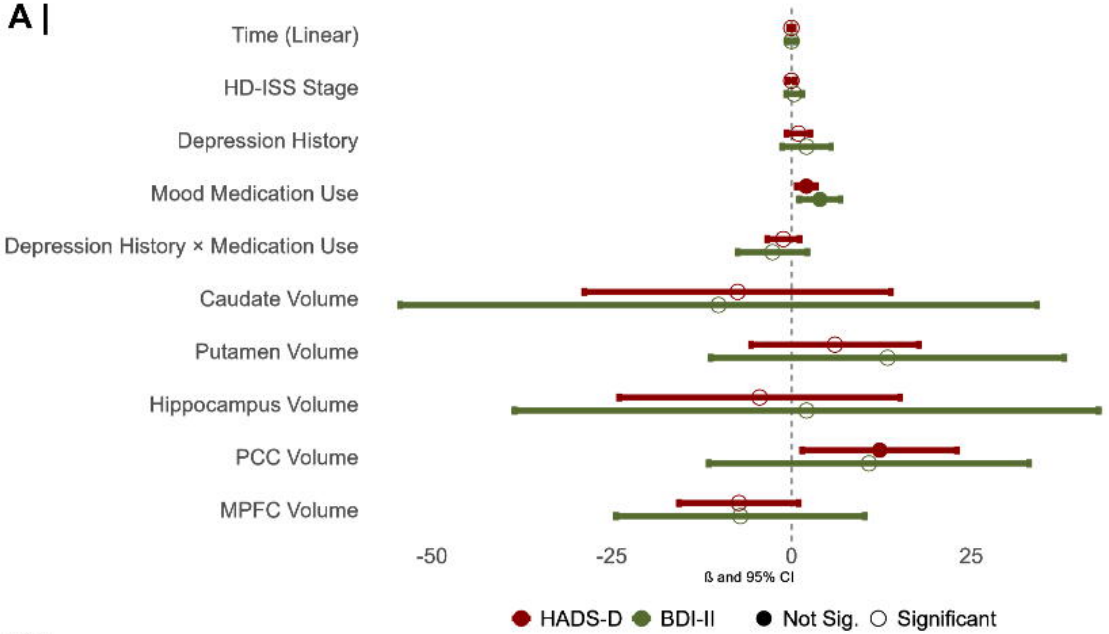
A |
Time (Linear)
HD-ISS Stage
Depression History
Mood Medication Use
Depression History × Medication Use
Caudate Volume
Putamen Volume
Hippocampus Volume
PCC Volume
MPFC Volume
-50
-25
0
25
ß and 95% CI
HADS-D
BDI-II
Not Sig.
Significant

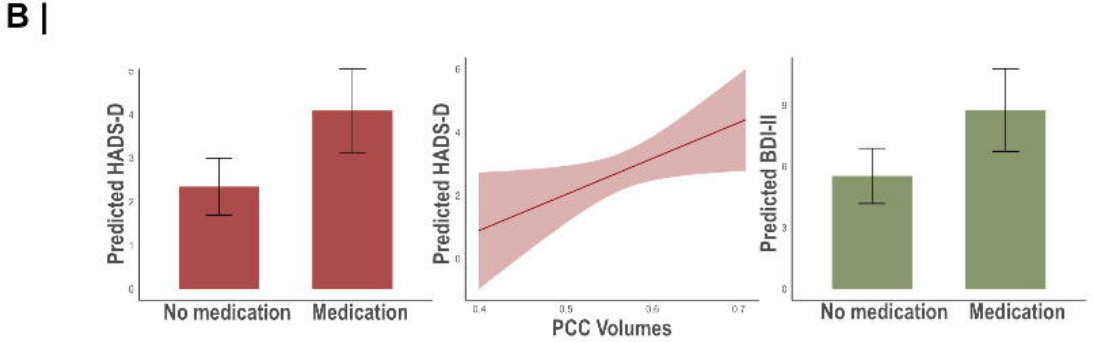
B |
Predicted HADS-D
No medication
Medication
Predicted HADS-D
PCC Volumes
Predicted BDI-II
No medication
Medication

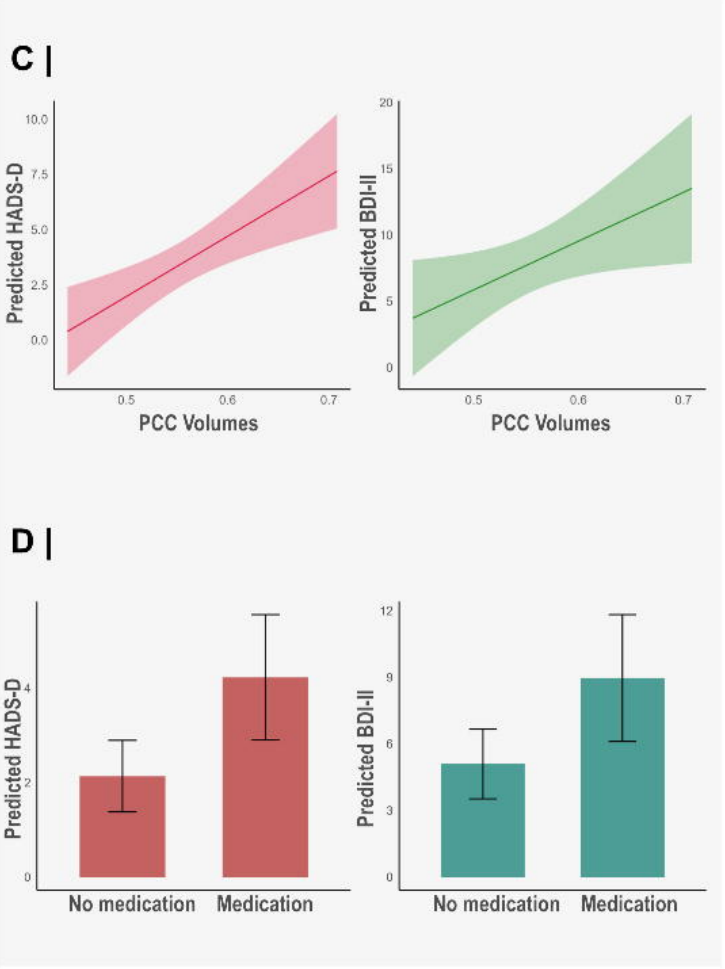
C |
Predicted HADS-D
PCC Volumes
Predicted BDI-II
PCC Volumes
D |
Predicted HADS-D
No medication
Medication
Predicted BDI-II
No medication
Medication

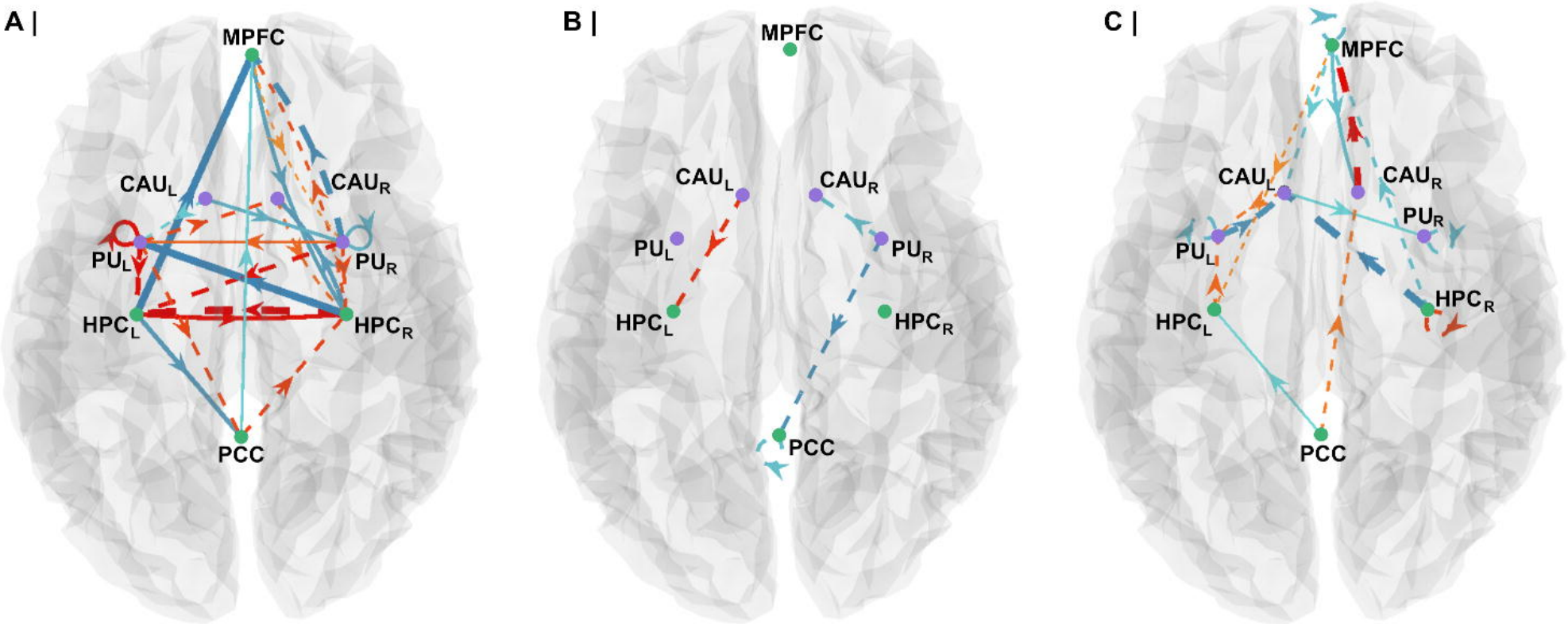
A |
MPFC
CAU$_L$
CAU$_R$
PU$_L$
PU$_R$
HPC$_L$
HPC$_R$
PCC
B |
MPFC
CAU$_L$
CAU$_R$
PU$_L$
PU$_R$
HPC$_L$
HPC$_R$
PCC
C |
MPFC
CAU$_L$
CAU$_R$
PU$_R$
PU$_L$
HPC$_R$
HPC$_L$
PCC

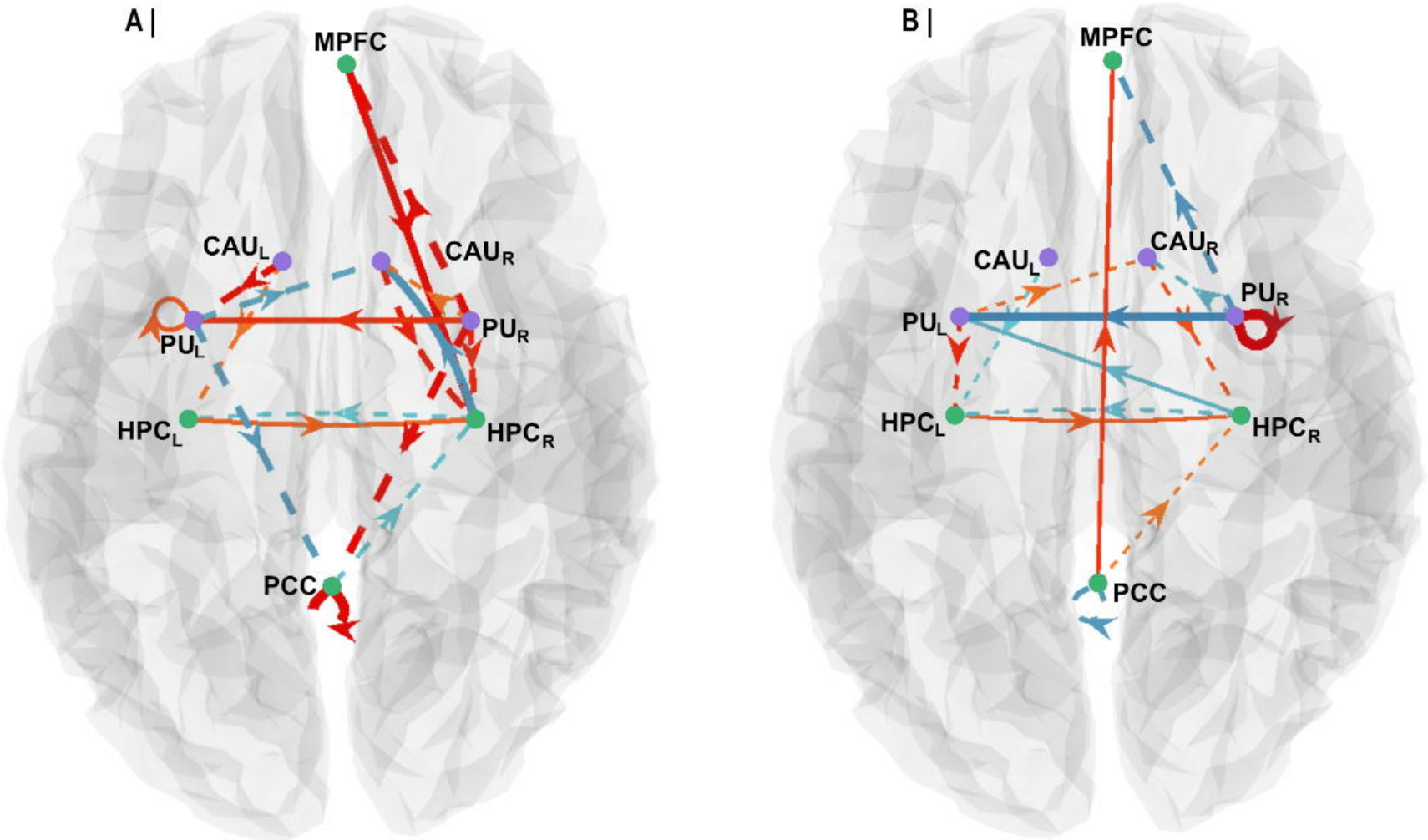
A |
MPFC
CAU$_L$
CAU$_R$
PU$_L$
PU$_R$
HPC$_L$
HPC$_R$
PCC
B |
MPFC
CAU$_L$
CAU$_R$
PU$_R$
PU$_L$
HPC$_L$
HPC$_R$
PCC

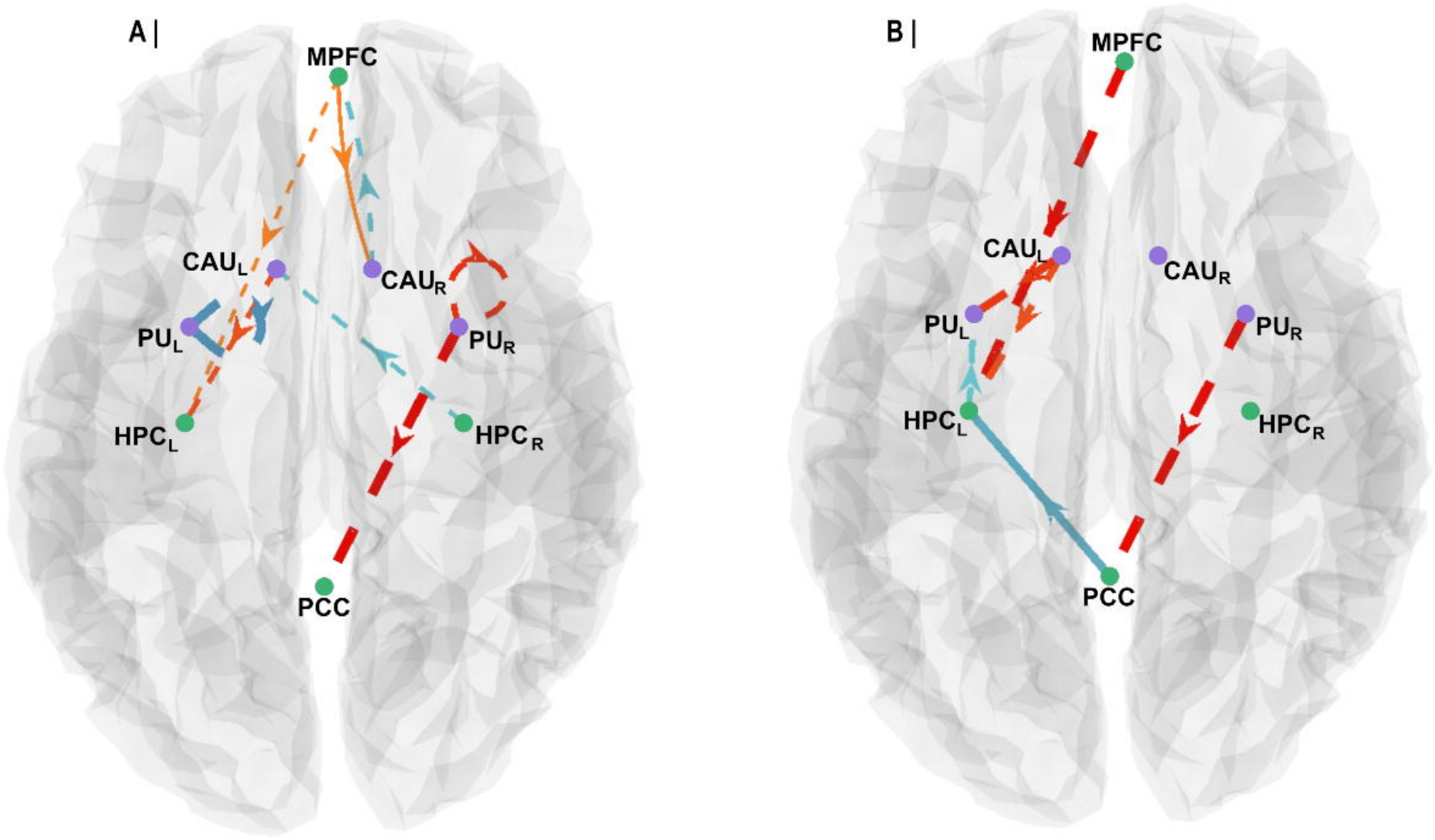
A |
MPFC
CAU$_L$
CAU$_R$
PU$_L$
PU$_R$
HPC$_L$
HPC$_R$
PCC
B |
MPFC
CAU$_L$
CAU$_R$
PU$_L$
PU$_R$
HPC$_L$
HPC$_R$
PCC